J Bioenerg Biomembr (2007) 39:499–505
DOI 10.1007/s10863-007-9117-7

Building an understanding of cystic fibrosis on the foundation of ABC transporter structures

Juan L. Mendoza · Philip J. Thomas

Published online: 13 December 2007
© Springer Science + Business Media, LLC 2007

Abstract Cystic fibrosis (CF) is a fatal disease affecting the lungs and digestive system by impairment of the Cystic Fibrosis Transmembrane Conductance Regulator (CFTR). While over 1000 mutations in CFTR have been associated with CF, the majority of cases are linked to the deletion of phenylalanine 508 (ΔF508). F508 is located in the first nucleotide binding domain (NBD1) of CFTR. This mutation is sufficient to impair the trafficking of CFTR to the plasma membrane and, thus, its function. As an ABC transporter, recent structural data from the family provide a framework on which to consider the effect of the ΔF508 mutation on CFTR. There are fifty-seven known structures of ABC transporters and domains thereof. Only six of these structures are of the intact transporters. In addition, modern bioinformatic tools provide a wealth of sequence and structural information on the family. We will review the structural information from the RCSB structure repository and sequence databases of the ABC transporters. The available structural information was used to construct a model for CFTR based on the ABC transporter homologue, Sav1866, and provide a context for understanding the molecular pathology of Cystic Fibrosis.

Keywords ABC transporters · CFTR · Cystic fibrosis

J. L. Mendoza · P. J. Thomas
Molecular Biophysics Graduate Program,
University of Texas Southwestern Medical Center,
6001 Forest Park Lane,
Dallas, TX 75390-9040, USA

P. J. Thomas (✉)
Department of Physiology,
University of Texas Southwestern Medical Center,
6001 Forest Park Lane,
Dallas, TX 75390-9040, USA
e-mail: Philip.Thomas@UTSouthwestern.edu

J. L. Mendoza
Department of Physiology,
University of Texas Southwestern Medical Center,
6001 Forest Park Lane,
Dallas, TX 75390-9040, USA

Domain organization of ABC transporters

CFTR is an ABC Transporter; a family of mechanochemical machines that couple ATPase activity to the movement of solutes across a membrane. They function as multi-domain proteins in a diverse number of configurations. The minimum functional unit of the family are two nucleotide binding domains (NBDs) and two transmembrane domains (TMDs) (Higgins 1992). ATP binding and hydrolysis at the NBDs transmit chemical work to domain rearrangements in the TMDs that allow for solute movement (Dassa and Hofnung 1985; Schmitt and Tampe 2002; Smith et al. 2002; Jones and George 2004).

The largest proteins in the family are the full-length transporters such as CFTR with all four domains on a single polypeptide chain (Higgins 1992). CFTR is 1480 amino acids long with a mass of approximately 170 kDa. At the N-terminus of the CFTR chain is the first TMD containing 6 transmembrane spans as typical for the family, followed by the first of the two NBDs. Unique to CFTR proteins is the insertion of a regulatory domain, the R-domain, following the first NBD. The R-domain is highly disordered and interacts with NBD1 in a phosphorylation dependent manner (Baker et al. 2007). Following the R-domain is a second TMD and then the second NBD (NBD2) at the C-terminus. This order of domain organization is the most prevalent for ABC transporters, however, there are predicted full-length transporters with other

domain organizations. In these cases, the N-terminus is initiated by a NBD domain and is continued alternating NBDs and TMDs. Half-transporters consist of a single TMD and NBD domain translated on a single polypeptide. Both eukaryotic as well as some microbial exporters, are can be arranged in this manner (Dawson et al. 2007). In this organization, half-transporters fulfill the ABC transporter minimum functional units by forming either homo or hetero-dimers. For the homodimeric bacterial transporter, Sav1866, the TMD is at the N-terminus followed by the NBD at the C-terminus. Similar to most full-transporters, half-transporters typically have the TMD at the N-terminus as is the case with Sav1866. However, proteins with the reverse TMD/NBD order also exist. The greatest number of ABC transporters, found in archae and bacteria, contain each domain on a separate chain and are expressed modularly. A single microbial operon typically contains the genes for each of the domains required to form the functional complex. Additionally, there are a small number of ABC transporters, which have two fused NBDs on a single polypeptide.

Nucleotide binding domains

There are 47,950 sequences included in the Pfam-A component for the NBDs of ABC transporters, PF00005 (Sonnhammer et al. 1997). The members which include two NBDs in a single polypeptide chain have both NBDs included in the multiple sequence alignment (MSA). Both CFTR NBD1 and NBD2 are included in the NBD MSA. Highlighting the high degree of conservation in the NBD region, the overall alignment has a percent identity of 26%. The NBDs of ABC transporters belong to the α/β class of proteins. Structural classification databases such as SCOP and CATH classify the NBDs as homologous and members of the P-loop containing nucleotide triphosphate hydrolases Superfamily (Murzin et al. 1995; Orengo et al. 1997). SCOP includes 25 different families including AAA-ATPases, Motor proteins, G proteins, and several kinase families. The P-loop, is also commonly known as the Walker A (GXXGXGKS/T) motif (Saraste et al. 1990). This is the glycine rich region with a conserved lysine and serine, which coordinate ligand binding of the ATP phosphates in other ATPases (Leslie et al. 2001). This sequence motif, along with the Walker B motif (Φ-Φ-Φ-Φ-D, where Φ is a hydrophobic residue), was one of the first identified and is highly conserved in different hydrolases regardless of the family (Walker et al. 1982; Jones and George 2004).

As of the writing of this review, there are 57 structures of ABC transporters or domains thereof. Most are of the NBDs (Table 1). In addition, there are many structures of the periplasmic solute binding proteins utilized by bacterial import ABC transporters. We do not further consider these domains here as they are not found in other ABC systems including CFTR. The structures available have been solved in apo, ligand bound, and mutant forms. The first structure of a core ABC transporter domain was published by Hung et al of the HisP NBD protein of the histidine permease (PDB 1B0U) (Hung et al. 1998). The initial structure was of monomeric HisP with ATP bound. The fold was unlike any other known structures at the time, but contained a core α/β domain similar to RecA (Story et al. 1992; Jones and George 1999). The P-loop is found in this subdomain, which also contains the Walker B motif. The Signature motif (LSGGQ) that identifies the ABC family was located in a smaller α-helical subdomain. The α-helical subdomain also contains the F508 residue in CFTR NBD1.

From biochemical studies, HisP was known to function as a dimer and the Signature motif was known to play a vital role in ATP binding and hydrolysis (Nikaido et al. 1997; Fetsch and Davidson 2002; Loo et al. 2002). Yet, in the crystal structure of the monomer, the Signature motif was not in contact distance with the single ATP molecule. This left unresolved the question as to how the Signature sequence contributed to the enzymatic function of NBD proteins. A model that resolved the conundrum was proposed placing the ATP in the interface of an NBD dimer (Jones and George 1999). The first suggestion this model might be correct came from a structure of Rad50. A member of the Structural and Maintenance of Chromosome (SMC) family of proteins; Rad50 is involved in DNA double-stranded break repair. Although, Rad50 is not an ABC Transporter, it was believed to be related to ABC transporters due to the similarity of fold (Hopfner et al. 2000). Rad50, makes a dimer pairing the Signature sequence from one chain to the Walker A and B motifs of the opposing chain with ATP sandwiched in between. In 2002, a structure of an ABC transporter NBD dimer (the Methanococcus jannashcii protein, MJ0796) was solved (Smith et al. 2002). The dimer was trapped by mutating the catalytic base (E171Q) (Moody et al. 2002). This structure revealed the Signature motif was involved in coordinating with the γ-phosphate of ATP in the dimeric form in a head to tail sandwich consistent with biochemical data (Moody et al. 2002; Fetsch and Davidson 2002). In this sandwich dimer the Signature motif residues of the second NBD complete the active site with the Walker A and B residues of the first NBD (Smith et al. 2002). This arrangement also explains the positive cooperativity of the ATPase.

ICL/NBD interactions

Alignments of transmembrane regions are more problematic due to the low level of conservation. In contrast to the large number of sequences available for the NBD align-

Table 1 ABC transporter structures in the research collaboratory for structural bioinformatics (RCSB) database

	Release Date	PDB	Protein	Resolution	Species
NBD Structures	Jun-05	1Z47	CysA	1.9	*Alicyclobacillus acidocaldarius*
	Sep-03	1OXX	GlcV G144A	1.45	*Sulfolobus solfataricus*
	Jun-03	1OXT	GlcV nucleotide free	2.1	*Sulfolobus solfataricus*
	Jun-03	1OXU	GlcV w/ ADP	2.1	*Sulfolobus solfataricus*
	Jun-03	1OXV	GlcV w/ AMP.PNP	2.1	*Sulfolobus solfataricus*
	Jun-03	1OXS	GlcV w/ iodide ions	1.65	*Sulfolobus solfataricus*
	Nov-99	1B0U	HisP w/ ATP	1.5	*Salmonella typimurium*
	Jun-03	1MT0	HlyB (467–707)	2.6	*Escherichia coli*
	Aug-06	2FFB	HlyB E631Q w/ ADP	1.9	*Escherichia coli*
	Aug-06	2FGK	HlyB E631Q w/ ATP	2.7	*Escherichia coli*
	Aug-06	2FFA	HlyB H662A w/ ADP	1.7	*Escherichia coli*
	Aug-06	2FGJ	HlyB H662A w/ ATP	2.6	*Escherichia coli*
	Jun-05	1XEF	HlyB w/ ATP	2.5	*Escherichia coli*
	Aug-06	2FF7	HlyB w/ADP	1.6	*Escherichia coli*
	Dec-03	1MV5	LmrA w/ ADP, ATP	3.1	*Lactococcus lactis*
	Dec-00	1G29	MalK	1.9	*Thermococcus litoralis*
	Sep-03	1Q1E	MalK	2.9	*Escherichia coli*
	Dec-04	1VCI	MalK w/ ATP	2.9	*Pyrococcus horikoshii*
	Aug-07	2QRR	metN	1.71	*Vibrio parahaemolyticus*
	Aug-07	2QSW	metN C-terminal domain	1.5	*Enterococcus faecalis*
	Jul-02	1L2T	MJ0796 E171Q Dimeric Structure	1.9	*Methanococcus jannaschii*
	Jul-01	1F3O	MJ0796 w/ ADP	2.7	*Methanococcus jannaschii*
	Nov-01	1GAJ	MJ1267	2.5	*Methanococcus jannaschii*
	Jul-01	1G6H	MJ1267 w/ ADP	1.6	*Methanococcus jannaschii*
	Feb-03	1G9X	MJ1267 w/ ADP	2.6	*Methanococcus jannaschii*
	May-06	2CBZ	MRP1-NBD1	1.5	*Homo sapiens*
	Nov-04	1V43	Multi-sugar transporter	2.2	*Pyrococcus horikoshii*
	Aug-04	1SGW	Putative	1.7	*Pyrococcus furiosus*
	Apr-07	2P0S	Putative	1.6	*Porphyromonas gingivalis*
	Sep-07	2IHY	Putative	1.9	*Staphylococcus aureus*
	Jan-06	2D3W	SufC	2.5	*Escherichia coli*
	Oct-06	2IXE	Tap1 D645N w/ ATP	2	*Rattus norvegicus*
	Oct-06	2IXF	Tap1 D645Q, Q678H w/ ATP	2	*Rattus norvegicus*
	Oct-06	2IXG	Tap1 S621A, G622V, D645N w/ ATP	2.7	*Homo sapiens*
	Sep-01	1JJ7	Tap1 w/ ADP	2.4	*Homo sapiens*
	Aug-02	1JI0	Thermatoga w/ ATP	2	*Sulfolobus solfataricus*
	Nov-04	1VPL	TM0544	2.1	*Thermotoga maritima*
CFTR NBD Structures	Nov-04	1XMJ	Human CFTR dF508 NBD1	2.3	*Homo sapiens*
	Nov-05	2BBT	Human CFTR dF508 NBD1 w/ two solublizing mutations	2.3	*Homo sapiens*
	Nov-05	2BBS	Human CFTR dF508 NBD1 w/ 3M	2.05	*Homo sapiens*
	Nov-05	2BBO	Human CFTR NBD1	2.55	*Homo sapiens*
	Nov-04	1XMI	Human CFTR NBD1—F508A w/ ATP	2.25	*Homo sapiens*
	Dec-04	1XFA	Murine CFTR—F508R	3.1	*Mus musculus*
	Dec-04	1XF9	Murine CFTR—F508S	2.7	*Mus musculus*
	Dec-03	1R0W	Murine CFTR NBD1	2.2	*Mus musculus*
	Dec-03	1R0Z	Murine CFTR NBD1 – phosphorylated w/ ATP	2.35	*Mus musculus*

Table 1 (continued)

	Release Date	PDB	Protein	Resolution	Species
	Dec-03	1R0W	Murine CFTR NBD1 apo	2.2	*Mus musculus*
	Dec-03	1R0Y	Murine CFTR NBD1 w/ ADP	2.55	*Mus musculus*
	Dec-03	1Q3H	Murine CFTR NBD1 w/ AMP.PNP	2.5	*Mus musculus*
	Dec-03	1R0X	Murine CFTR NBD1 w/ ATP	2.2	*Mus musculus*
	Dec-03	1R10	Murine CFTR NBD1 w/ ATP	3	*Mus musculus*
TMD/NBD complex structures	Mar-07	2ONJ	Sav1866 w/ AMP.PNP	3.4	*Staphylococcus aureus*
	Sep-06	2HYD	Sav1866 w/ ADP	3	*Staphylococcus aureus*
	Aug-07	2QI9	BtuCD in complex with BtuF	3.2	*Escherichia coli*
	May-02	1L7V	BtuCD w/ cyclo-tetrametavanadate	3.2	*Escherichia coli*
	Mar-07	2ONK	ModBC in complex with ModA	3.1	*Archaeoglobus fulgidus*
	Jan-07	2NQ2	HI1470/1	2.4	*Haemophilus influenza*

ments in Pfam, only 6,419 transmembrane sequences are in the MSA of ABC transporter TMDs, PF00664 (Sonnhammer et al. 1997). The average percent identity of the sequences in the alignment is only 14%. Thus, even with the most robust methodologies, alignments of transmembrane regions are susceptible to inaccuracies and motifs are more difficult to identify. One such sequence in the intercellular loops connecting the TM segments of ABC transporter uptake proteins is the EAA-X(3)-G-X(9)-LP motif (Doige and Ames 1993; Saurin and Dassa 1994; Biemans-Oldehinkel et al. 2006). This motif is not ubiquitous throughout the family (Dassa and Hofnung 1985; Schmitt and Tampe 2002; Biemans-Oldehinkel et al. 2006). Thus, quality assessments of the transmembrane domains are not possible due to low conservation across the family in these regions consistent with their role in mediating movement of a wide variety of structurally diverse solutes.

Of the available ABC transporter structures, only six structures, which include the proteins BtuCD, HI1470/1, ModBC, and Sav1866 contain the NBDs in complex with the transmembrane domains. Structures of a fifth protein, MsbA (PDB 1Z2R and 1PF4), have been retracted due to software problems in generating the structure models (Chang and Roth 2001; Reyes and Chang 2005; Chang et al. 2006; Matthews 2007). BtuCD is an ABC vitamin B12 importer and was the first ABC transporter to be crystallized with both NBD and TMD components (PDB 1L7V) (Locher et al. 2002). Unlike other ABC transporters, each half of the TMD region of BtuCD has 10 transmembrane spans with 4 ICLs. Moreover, BtuCD has different ICL/NBD interactions from the other known intact transporters. A single TMD interacts with a single NBD by way of three of the four ICLs (Fig. 1a). In addition, the N-terminus packs against the outside of the α-helical subdomain. The first ICL only has two residues within contact distance of the NBD and contacts the α-helical subdomain. ICL2 is not in a close enough proximity to directly interact with either of the two NBDs. The nearest atom of the NBD to ICL2 is approximately 7.7 angstroms. ICL3 has the greatest amount of interaction surface area and interacts with the NBD between both the α-helical and α/β subdomains. In this region of the interface, the ICLs and NBDs share both polar and hydrophobic interactions. The fourth ICL (ICL4) sits above the α-helical subdomain centered between the N and C-termini of the TMD and ICLs 1 and 3.

More prototypical of the transporter family are ModBC and Sav1866. ModBC (PDB 2ONK) is a modular archaeal importer, which has 6 transmembrane spans and two ICLs in each of the TMDs (Hollenstein et al. 2007). Unlike the BtuCD structure in which a single TMD interacts with a single NBD, in ModBC, each of the N-termini cross over to the opposing NBD (Fig. 1b). The N-terminus of each TMD is positioned within 4.4 angstroms of the outer face of the opposing NBD. ICL1 makes contacts with the N and C-termini of the opposing TMD and does not come in contact with either of the NBDs. ICL2 is positioned in the groove between the α/β and α-helical subdomains. The C-terminus of the ModBC TMDs rest above the NBD α-helical subdomains but are not within contact distance of the NBDs.

A third arrangement is seen in Sav1866 (2HYD PDB), a bacterial multi-drug transporter containing a single TMD and NBD on a single polypeptide (Dawson and Locher 2006). Of the four, structures with the complex of TMD and NBDs, Sav1866 is the only half-transporter. The

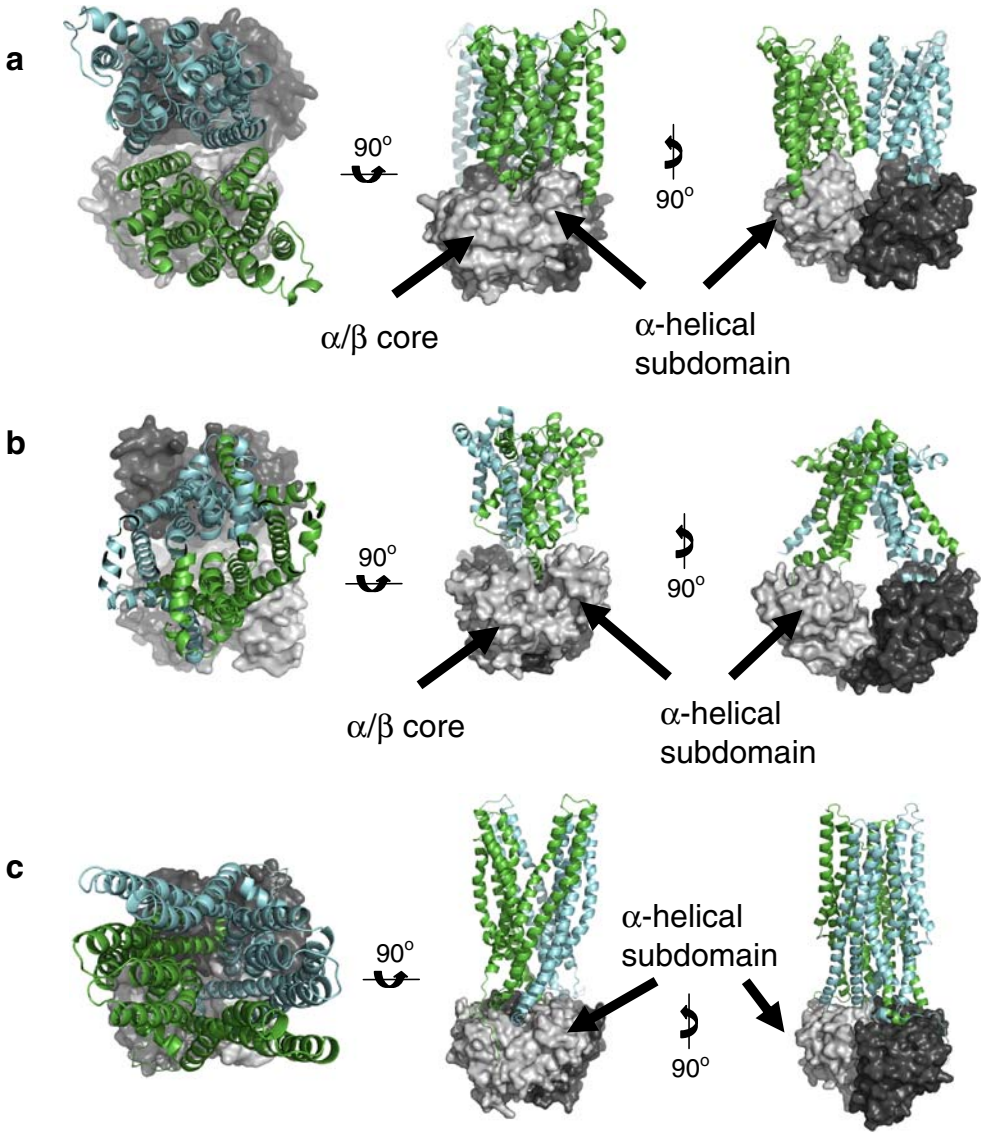

Fig. 1 TMD/NBD interactions in intact ABC transporter structures (Pdb: 1L7V, 2ONK and 2HYD). **a.** The structure of BtuCD. NBDs are represented in surface models in *light gray* and *dark gray*. Ribbon representations of the TMDs with their ICLs *cyan* and *green*. Each of the BtuC TMDs contain ten transmembrane spans and four ICLs. Three of the four ICLs are within contact distance of the proximal NBD. In this structure, ICLs from one TMD interact with a single NBD. *Left* Top view from the perspective of the membrane. *Center* Rotation by 90° in the plane of the page from the prior view. *Right* Side view of the prior view by rotating 90° out of the plane of the page. **b.** The structure of ModBC. NBDs are represented in surface models in *light gray* and *dark gray*. Ribbon representations of the TMDs are in *cyan* and *green*. Each of the ModB TMDs contain six transmembrane spans with 2 ICLs. In this structure, two ICLs from one TMD interact with a single NBD and the N-terminus of each of the TMDs "swap" and are within contact distance of the distal NBD. *Left* Top view from the perspective of the membrane. *Center* Rotation by 90° in the plane of the page from the prior view. *Right* Side view of the prior view by rotating 90° out of the plane of the page. **c.** The structure of Sav1866. NBDs are represented in surface models in *light gray* and *dark gray*. Ribbon representations of the TMDs are in *cyan* and *green*. Each of the Sav1866 TMDs contain six transmembrane spans with 2 ICLs. In this structure, both ICLs from one TMD interact with each of the two NBDs. *Left* Top view from the perspective of the membrane. *Center* Rotation by 90° in the plane of the page from the prior view. *Right* Side view of the prior view by rotating 90° out of the plane of the page

Sav1866 TMD has six transmembrane spans located at the N-terminus of the protein. The NBD is at the C-terminus. In the Sav1866 homodimer structure, ICLs form interactions with both NBDs (Fig. 1c). Thus, each of the NBDs are contacted by both the TMDs. ICL1 sits directly above the P-loop interacting with its own NBD at the α/β subdomain. The interface has approximately 132 angstroms^2 of surface area with a near equal number of polar and non-polar atoms, 56% and 44%, respectively. The ATP adenine ring is within 4.2 angstroms of ICL1. Additionally, ICL1 interacts with the opposing NBD above the α-helical subdomain near the Signature motif. This interface has approximately 187 angstroms^2 of surface area with nearly equal number of polar to non-polar atoms, 46% and 54%, respectively. ICL2

solely interacts with the NBD of the opposing dimer chain. The nidus of the ICL2/NBD interaction occurs at the groove between the α/β and α-helical subdomains of the dimer NBD chain. There are approximately 725 angstroms^2 of surface area at the ICL2/NBD interface. Furthermore, this interface is strongly characterized by a hydrophobic interface with a 32% and 68% polar to non-polar atoms, respectively. Sav1866 is the closest homologue of CFTR for which a structure is available.

A model for CFTR

The large majority of CF patients have the disease linked to the deletion of phenylalanine 508 in the N-terminal NBD1 of CFTR. The ΔF508 CFTR misfolds at physiological conditions and does not traffic efficiently beyond the endoplasmic reticulum as monitored by complex glycosylation (Cheng et al. 1990). The mutant also affects the isolated NBD1 (Thibodeau et al. 2005). In the cell, ΔF508 CFTR is targeted for degradation (Lukacs et al. 1994). Notably, electrophysiological studies indicate that when ΔF508 CFTR is temperature-rescued the channel has activity. Thus, the primary cause of this form of CF disease is due to the disruption of the folding pathway of CFTR. Understanding the structural perturbations, which occur due to the deletion of F508 is of great interest and practical importance as correcting CFTR's inability to reach the plasma membrane should be of therapeutic benefit. Because there is no structure of full-length CFTR, models provide important insight into elucidating the interactions within CFTR and the effect of disease-causing mutations.

At present there are structures for the first NBD (NBD1) of CFTR (Table 1). Also available is a ΔF508 NBD1 containing mutants that enable folding. The structure of NBD2 has yet to be determined. However, like other ABC transporters, the two NBDs of CFTR are expected to interact and bind two molecules of ATP (Vergani et al. 2005). If NBD1/NBD2 forms such a sandwich dimer then only one of these two sites will be enzymatically active, because the catalytic glutamate is absent in the Walker B motif in CFTR NBD1 (Lewis et al. 2004). Mutations at three positions (G550, R553, and R5550) in NBD1 have been found to correct the folding defect of ΔF508 solubility (Dork et al. 1991; Teem et al. 1993, 1996; DeCarvalho et al. 2002). All three second site suppressor mutations are located in the α-helical subdomain. A crystal structure has been solved of ΔF508 NBD1 containing these three suppressor mutations (Lewis et al. 2005). Comparison of the structures for wild type NBD1 and the ΔF508 NBD1 with the three solubilizing mutations do not reveal any significant rearrangements. Alignments of the mutant

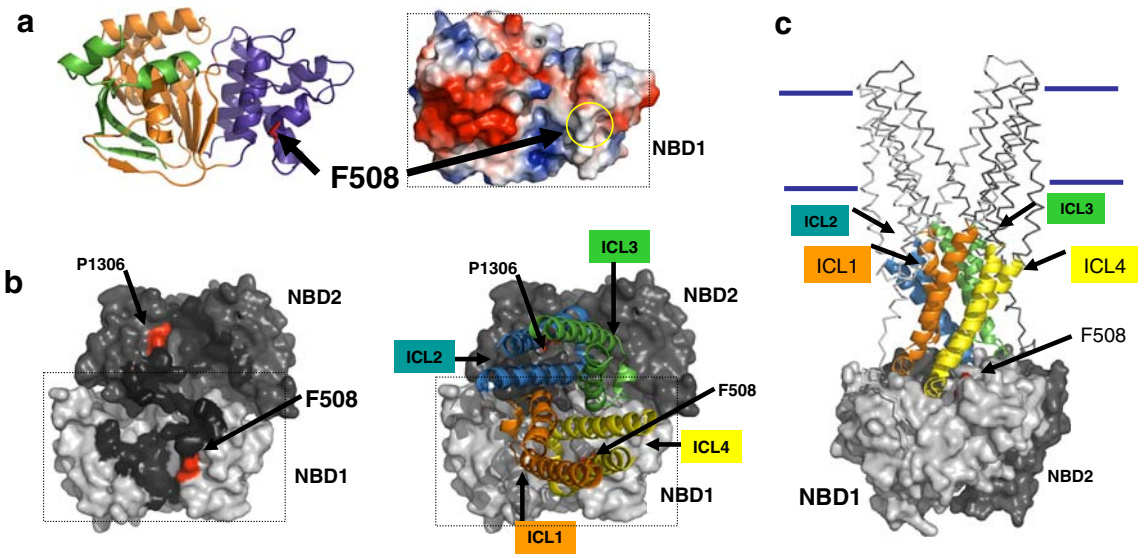

Fig. 2 Model of TMD and NBD interactions in CFTR (Based on: 1R0W and 2HYD). **a.** Structure of CFTR NBD1 looking from the perspective of the membrane plane. *Left* Ribbon representation of the CFTR NBD1. The N-terminal region is colored in *green*. The Walker A and B motifs are located in the α/β-core subdomain *orange*. The Signature "LSGGQ" and F508 residue *red* are located in the α-helical subdomain *dark blue*. *Right* Electrostatic surface representation with *negative-red* and *positive-blue*. The hydrophobic-white 508 position is exposed and is indicated by the yellow circle. **b.** The Sav1866 structure was used to produce a working model for CFTR. The relative interactions of the NBDs, the ICLs, and specific CFTR residues are indicated. The two NBDs dimerize with the two ATPs (not shown) sandwiched between the interface, analogous to the MJ0796 sandwich dimer structure. *Left* The NBD sandwich dimer is shown stripped of the TMDs and connecting ICLs. The surfaces covered by the ICLs are shown in black and the surface exposed positions of F508 and P1306 (predicted) are shown in *red*. *Right* Same view with the ICLs in place. ICL4 sits in a groove on the surface of NBD1 between the α-helical subdomain and the α/β-core and near the F508 position (partially hidden). **c.** A side view of the CFTR model

structure against wild type NBD1 are within 0.6 angstroms RMS deviation. In addition to the effect of the disease causing mutation on isolated NBD1 folding, the structures place the ΔF508 mutation on the surface of the domain in a position predicted to interact with the ICLs in other ABC transporters. In this regard, Lewis et al propose one effect of ΔF508 CFTR is the disruption of interdomain interactions with the membrane spans (Lewis et al. 2004).

A current open question is what is the nature of this interface. That is how do the ICLs interact with the NBDs in CFTR? If CFTR is arranged like the exporter, Sav1866, CFTR ICL2 (predicted 242 to 307) and ICL3 (predicted 930 to 990) would interact with NBD2 (Seibert et al. 1996; Wigley et al. 1998). CFTR ICLs 1 (predicted 141–194) and 4 (predicted 1037 to 1095) would interact with NBD1 (Cotten et al. 1996; Wigley et al. 1998) (Fig. 2). In this model, CFTR ICL4 makes contacts with the F508 position of NBD1 while ICL2 makes contacts with the equivalent P1306 position in NBD2. The Sav1866-based model predicts CFTR ICL4 will have the largest contribution to the ICL/NBD interaction surface area of NBD1. Consistent with this prediction, biochemical studies showed CF-causing mutations in ICL4 altered the gating of the channel in response to stimuli (Cotten et al. 1996).

Due to the lack of efficient expression systems to yield large amounts of CFTR, and the presence of a large disordered regions in the R-domain; CFTR has proven to be a difficult target for structural analysis. In spite of this difficulty, significant progress has been made in understanding the molecular pathology. The availability of CFTR NBD1 structures in addition to structures of intact homologous transporter proteins, allows construction of structural models suggesting specific interactions between the ICLs and NBDs. Zolnerciks et al. have recently reported biochemical experiments providing for a Sav1866-like TMD/NBD interactions with another human ABC transporter, the multi-drug transporter P-glycoprotein (Zolnerciks et al. 2007). Thus, models built on structural and biochemical studies can generate testable hypothesis that lead to a deeper understanding of the mechanism of CF-causing mutations.

Acknowledgements This work was supported by grants from the Welch Foundation (I-1284), the CF Foundation, and NIH (DK49835) to PJT.

References

Baker JM, Hudson RP, Kanelis V, Choy WY, Thibodeau PH et al (2007) Nat Struct Mol Biol 14(8):738–745
Biemans-Oldehinkel E, Doeven MK, Poolman B (2006) FEBS Lett 580(4):1023–1035
Chang G, Roth CB (2001) Science 293(5536):1793–1800
Chang G, Roth CB, Reyes CL, Pornillos O, Chen YJ et al (2006) Science 314(5807):1875
Cheng SH, Gregory RJ, Marshall J, Paul S, Souza DW et al (1990) Cell 63(4):827–834
Cotten JF, Ostedgaard LS, Carson MR, Welsh MJ (1996) J Biol Chem 271(35):21279–21284
Dassa E, Hofnung M (1985) Ann Inst Pasteur Microbiol 136A (3):281–288
Dawson RJ, Locher KP (2006) Nature 443(7108):180–185
Dawson RJ, Hollenstein K, Locher KP (2007) Mol Microbiol 65 (2):250–257
DeCarvalho AC, Gansheroff LJ, Teem JL (2002) J Biol Chem 277 (39):35896–35905
Doige CA, Ames GF (1993) Annu Rev Microbiol 47:291–319
Dork T, Wulbrand U, Richter T, Neumann T, Wolfes H et al (1991) Hum Genet 87(4):441–446
Fetsch EE, Davidson AL (2002) Proc Natl Acad Sci U S A 99 (15):9685–9690
Higgins CF (1992) Annu Rev Cell Biol 8:67–113
Hollenstein K, Frei DC, Locher KP (2007) Nature 446(7132):213–216
Hopfner KP, Karcher A, Shin DS, Craig L, Arthur LM et al (2000) Cell 101(7):789–800
Hung LW, Wang IX, Nikaido K, Liu PQ, Ames GF et al (1998) Nature 396(6712):703–707
Jones PM, George AM (1999) FEMS Microbiol Lett 179(2):187–202
Jones PM, George AM (2004) Cell Mol Life Sci 61(6):682–699
Leslie EM, Deeley RG, Cole SP (2001) Toxicology 167(1):3–23
Lewis HA, Buchanan SG, Burley SK, Conners K, Dickey M et al (2004) EMBO J 23(2):282–293
Lewis HA, Zhao X, Wang C, Sauder JM, Rooney I et al (2005) J Biol Chem 280(2):1346–1353
Locher KP, Lee AT, Rees DC (2002) Science 296(5570):1091–1098
Loo TW, Bartlett MC, Clarke DM (2002) J Biol Chem 277 (44):41303–41306
Lukacs GL, Mohamed A, Kartner N, Chang XB, Riordan JR et al (1994) EMBO J 13(24):6076–6086
Matthews BW (2007) Protein Sci 16(6):1013–1016
Moody JE, Millen L, Binns D, Hunt JF, Thomas PJ (2002) J Biol Chem 277(24):21111–21114
Murzin AG, Brenner SE, Hubbard T, Chothia C (1995) J Mol Biol 247(4):536–540
Nikaido K, Liu PQ, Ames GF (1997) J Biol Chem 272(44):27745–27752
Orengo CA, Michie AD, Jones S, Jones DT, Swindells MB et al (1997) Structure 5(8):1093–1108
Reyes CL, Chang G (2005) Science 308(5724):1028–1031
Saraste M, Sibbald PR, Wittinghofer A (1990) Trends Biochem Sci 15 (11):430–434
Saurin W, Dassa E (1994) Protein Sci 3(2):325–344
Schmitt L, Tampe R (2002) Curr Opin Struct Biol 12(6):754–760
Seibert FS, Linsdell P, Loo TW, Hanrahan JW, Riordan JR et al (1996) J Biol Chem 271(44):27493–27499
Smith PC, Karpowich N, Millen L, Moody JE, Rosen J, et al (2002) Mol Cell 10(1):139–149
Sonnhammer EL, Eddy SR, Durbin R (1997) Proteins 28(3):405–420
Story RM, Weber IT, Steitz TA (1992) Nature 355(6358):318–325
Teem JL, Berger HA, Ostedgaard LS, Rich DP, Tsui LC et al (1993) Cell 73(2):335–346
Teem JL, Carson MR, Welsh MJ (1996) Recept Channels 4(1):63–72
Thibodeau PH, Brautigam CA, Machius M, Thomas PJ (2005) Nat Struct Mol Biol 12(1):10–16
Vergani P, Lockless SW, Nairn AC, Gadsby DC (2005) Nature 433 (7028):876–880
Walker JE, Saraste M, Runswick MJ, Gay NJ (1982) EMBO J 1 (8):945–951
Wigley WC, Vijayakumar S, Jones JD, Slaughter C, Thomas PJ (1998) Biochemistry 37(3):844–853
Zolnerciks JK, Wooding C, Linton KJ (2007) FASEB J 21(14):3937–3948